Article

Fragment impact of cased explosive

Wing Cheng*, Scott Langlie**, Shan Lin**, and Shigeru Itoh***

Fragment impact of cased explosives was studied by experimental testing and numerical modeling. The objective was to obtain a better understanding of detonation phenomenon and to determine if case explosive of a specific warhead configuration will detonate when subjected to impact of an 80-gram Fragment Simulated Projectile (FSP) at various impact velocities. The stress was measured on the backside of the steel plate in a ballistic test using an experimental technique. Relationship between impact velocity against a warhead casing and pressure induced between the warhead casing and the explosive was determined. Numerical modeling of this experiment was performed using a hydrodynamic code, to validate the results of the experiment in predicting the impact pressure on the backside of the steel plate. At the end, numerical modeling of a 80 FSP impacting a steel plate, which was backed by unconfined cased H6 explosive was used to predict detonation of the explosive. Of the impact velocities studied, ranging from 235 m/s to 2,225 m/s, only impact velocity of 2,225 m/s resulted in severe detonation.

1. Introduction

This paper reports the results of validation of DYNA2D, in numerical modeling of a 80-gram FSP impacting a steel plate, which was backed by polymethyl methacrylate material, commonly known as Plexiglas. The steel plate was used to simulate a steel warhead casing, and Plexiglas, an inert explosive material. Impact pressure was determined on the backside of the steel plate when the target was impacted by FSPs, fired at various velocities. Numerical prediction was then compared with results obtained from ballistic test, determining a correlation between the numerical and experimental data.

Ballistic test firings were performed at the Dayton Impact Research Institute of the University of Dayton using a 50-mm compressed gas/gunpowder gun. The target was impacted by steel 80-gram FSP's fired at velocities ranging from 235 to 1,067 m/s, for a series of seven shots. Two types of gauges were embedded in the target, namely Manganin pressure gauge and Constantan strain gauge. The strain gauge was used to monitor the lateral strain produced by the impact of the FSP on a steel-Plexiglas target. Pressure histories resulting from the fragment impact were recorded for various impact velocities. This paper compares the numerical prediction using DYNA2D numerical model with data obtained from ballistic test.

The numerical model was later extended to predict detonation of explosive by impact of an 80-gram FSP impacting a steel plate backed by unconfined cast H6 explosive. The objective was to gain a better understanding of the detonation phenomenon of cased explosive and to determine if the H6 explosive will detonate when subjected to various impact velocities. Eight numerical experiments were performed using DYNA2D, representing 8 different impact velocities ranging from 235 to 2,225 m/s. A reactive model developed previously by the authors for the H6 explosive was used to predict detonation of the explosive.

Received : May 17, 2002
Accepted : September 6, 2002
*MechComp, Inc. Sunnyvale, California, USA
**FMC Advanced Systems Center Minneapolis, Minnesota, USA
***Shock Wave and Condensed Matter Research Center Kumamoto University, Kurokami Kumamoto, JAPAN

2. Fragment impact experiment

The experiment was performed to determine the relationship between the impact velocity of the 80-gram FSP against a warhead casing and the pressure induced between the warhead casing and the explosive. Figure 1 shows the simulated target assembly. Stress measurement was made in a 4340 steel plate, backed by Plexiglas target, by embedding Manganin stress and Constantan strain gauges 0.15 cm into the Plexiglas which was behind the steel plate. The target assemblies were impacted by 4340 steel FSP's at velocities ranging from 235 to 1,067 m/s in seven shots. The upper limit of the muzzle velocity of the gun was 1,067 m/s, given the required launch package mass. Strain gauge output (ΔR/Ro) was used to determine the lateral strain in the target by assuming the impact geometry axially symmetric. Measured values of (ΔR/Ro) from the Manganin gauge were analyzed by considering the contribution from the lateral strain produced in the target. The stress values inferred from this analysis were compared to the ($\Delta R/R_o$) of the Manganin gauge. The uncorrected stress values were about four to five times the corrected value [1].

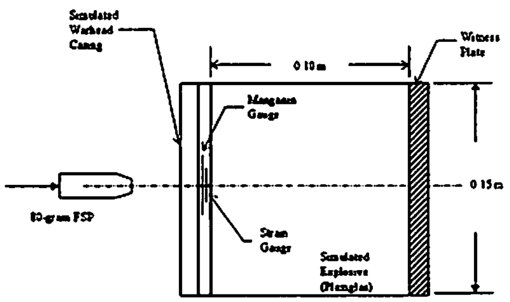

Fig. 1 Ballistic Impact Target

The 80-gram FSP and the 1.9 cm steel plate were made of the same 4340 steel which was heat-treated to a specified hardness of Rc=30+/-1. The steel plate was cut to 10.2-by 10.2-cm pieces to be used as targets. The launch package is shown in Fig. 2. Brass foil electrodes of 0.003-cm thick were soldered to the Manganin and strain gauges. One Manganin and one strain gauge were glued to the top of the 15.2- by 15.2-cm Plexiglas piece that was 10.2-cm thick. The 1.9-cm thick 10.2- by 10.2-cm 4340 steel plate was glued on the top of the gauge and Plexiglas assembly. Figure 3 shows the entire target assembly placed between two 2.5-cm thick steel plates. The front steel plate had a 3.18-cm hole for the entry of the FSP during the shot. This steel plate served as a stripper for the lexan sabot. Each FSP impacted the steel target at exactly the same point, with zero yaw and zero pitch.

Projectiles were launched using compressed gas for the first three low-velocity shots. All other projectiles were launched using gunpowder to generate the propelling force. The output of the 48-ohm Manganin gauge was recorded on a dual-beam Tektronix scope as ΔV using a Manganin gauge pulser.

The pulser was triggered by one of the velocity

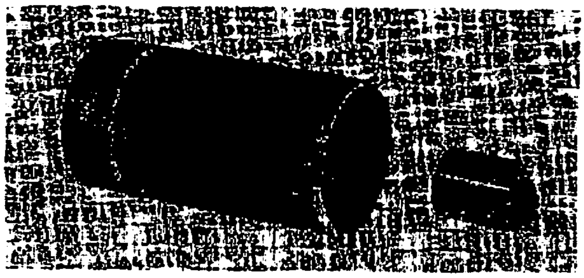
Fig. 2 Projectile assembly showing lexan sabot on the left and FSP on the right

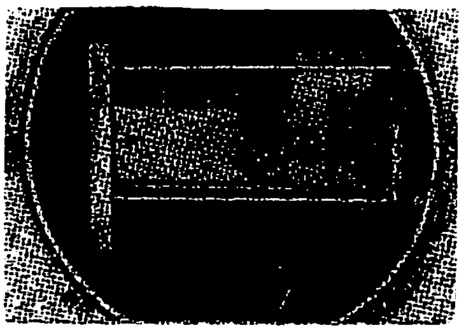
Fig. 3 Assembled target in target chamber

pins in the gun barrel. The Tektronix scope was triggered using a delay unit with a predetermined delay with respect to the velocity pin. The output from the strain gauge and the Manganin gauge were recorded on the same Tektronix scope. Both amplifiers, one for the Manganin gauge and the other for the strain gauge, were run with the same time basis. This technique allowed correlation of the Manganin and strain gauges records for the same instant of time during the impact event.

Figure 4 shows a typical oscilloscope trace for the two gauges.

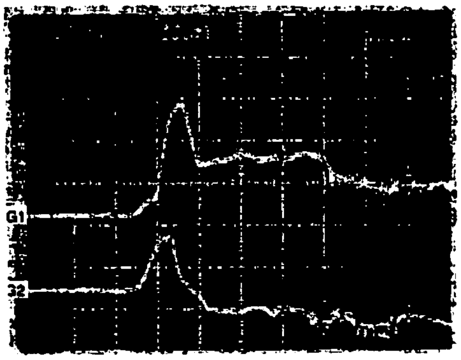

Fig. 4 Oscilloscope traces of manganin (G1) and strain (G2) gauges (scales for G1 and G2; 0.1 V/div., 10 microseconds/div.)

3. Experimental results

In the low velocity shots, no physical change in the Plexiglas was noticed. For shots at medium velocity, the top sheet of Plexiglas was shattered into 5-cm pieces. In the high velocity shots, all of the Plexiglas was shattered into pieces. Complete penetration (V50) through the steel plate occurred at a velocity of 1,067 m/sec.

The Tektronix scope records of the Manganin and Strain gauges in five of the nine experiments conducted were very clear. The rise time s for both stress and strain gauge records are in the 3- to 5-microsecond range.

4. Data analysis

The ΔV values of the Manganin and Strain gauges were converted to $\Delta R/R_o$ to obtain stress and strain corresponding to each impact velocity (Rosenberg and Strader, 1985 [2]). The data on $\Delta R/R_o$ of the gauges is summarized in Table 1. The values of $\Delta R/Ro$ on the Manganin gauge show a systemic increase with the impact velocity as the impact velocity increased from 235 to 520 m/sec, but for velocities higher than that, the values of $\Delta R/R_o$ are about half of the lower shots. This may be caused by the gauge not being directly below the impact area, and the impact face of the FSP is not round and, therefore, does not produce a spherical stress wave into the impacted target.

Table 1 Manganin and strain gauge results on $\Delta R/R_o$

Shot No.	Impact Velocity (m/sec)	Manganin Gauge		Strai Gauge	
		ΔV	$\Delta R/R_o$	ΔV	$\Delta R/R_o$
7-1230	235	0.18	0.0160	0.090	0.0125
7-1228	371	0.25	0.0175	0.120	0.0167
7-1225	520	0.34	0.0235	0.160	0.0222
7-1226	642	0.51	0.0347	0.085	0.0118
7-1227	794	0.58	0.0388	0.086	0.0119
7-1229	961	0.64	0.0435	0.320	0.0445
7-1231	1,067	0.97	0.0659	0.430	0.0597

Table 2 Lateral strain, corrected stress and uncorrected stress results

Shot No.	Impact Velocity (m/sec)	Lateral Strain ($-\varepsilon_l$)	Corrected Stress (kbar)	Un-corrected Stress (kbar)
7-1230	235	0.0063	1	6
7-1228	371	0.0084	2	9
7-1225	520	0.0111	3	12
7-1226	642	0.0059	11	16
7-1227	794	0.0060	12.4	18
7-1229	961	0.0223	2.8	20
7-1231	1,067	0.0299	9.7	28

5. Determination of stress and strain

The impact geometry in the present experiments closely approximates axial symmetry, with the symmetry axis in the impact direction. The dimensions of the FSP and the nature of impact are such that state of strain in the target is not uni-axial as experienced in-plate impact shock wave experiments. Therefore, we need to first obtain the lateral strain in the target from the strain gauge data. The calibration of the Manganin stress gauge ($\Delta R/Ro$ versus stress) in-plate impact experiments is normally done when the lateral strains in the target are zero. Thus, in order to use the Manganin gauge calibration, we must subtract the component of $\Delta R/R_o$ that is due to the lateral strains in the target.

Analysis technique developed by Rosenberg, et al in 1984 [3] was adopted to make correction of the measured stresses. Table 2 shows the values for the lateral strain, ε_L, derived from $\Delta R/R_o$ of the strain gauge. These values of ε_L and the corresponding $\Delta R/R_o$, of the Manganin gauge are substituted in Rosenberg's formulation to obtain the axial stress.

Corrected stress values are lower by a factor of about five compared to the uncorrected values. This is a clear evidence of the role of lateral strain in the response of the Manganin gauge. The lower lateral strain values for shots 1 and 2 are due to relatively lower strain gauge response recorded in these two shots.

6. Modeling of simulated cased explosive (plexiglas)

Before detonation of explosive for an actual configuration was modeled, a series of simulations were performed to validate the numerical tools for predicting the pressure resulting from the impact of an 80-gram FSP on a steel/Plexiglas laminated target. A two-dimensional Lagrangian finite element computer codes, DYNA2D (Hallquist, 1988 [4]), was used. The pressure pulse loading onto the Plexiglas material was of particular interest. Figure 5 shows the finite element model for the DYNA2D simulations. The projectile was modeled using a 4340-steel rod with a 2.23-cm diameter. The projectile had a tapered tip, which was 2.74-cm long, and a mass of 80 grams. The target plate was also modeled using 4340 steel with a 15.2-cm diameter and was 1.90-cm thick. The Plexiglas plate was modeled using Plexiglas material properties, a 15.2-cm diameter target, and was 10.2-cm thick.

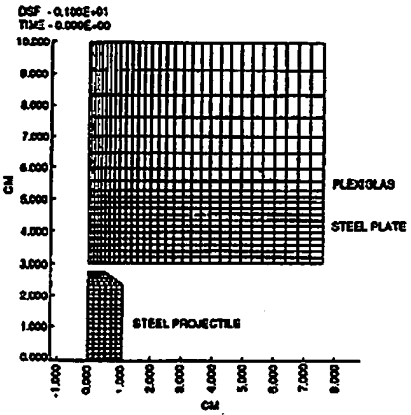

Fig. 5 Impact finite element model with Plexiglas

Figure 6 shows the time history for the impact velocity of 1,067 m/sec of the impact pressure behind the steel plate. The maximum calculated impact pressure is 13.15 kbar, which occurred at approximately 7 micro-seconds. Fragment impact simulations were performed for seven different velocities of 235, 371, 520, 642, 794, 961 and 1,067 m/sec.

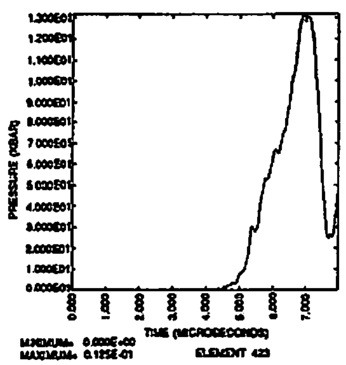

Fig. 6 Pressure history plot (V = 1,067 m/sec)

7. DYNA2D validation results

Figure 7 shows the impact pressures versus impact velocity obtained from the DYNA2D calculations and the ballistic test measurement. In actual test results, the Plexiglas blocks were shattered into many pieces, which the numerical model did not simulate. Complete penetration of the steel plate occurred at a velocity of 1,067 m/sec. Good correlation was observed between the results obtained from the numerical simulations and the ballistic tests for low impact-velocity regime, large discrepancy resulted at high impact velocity. It is clear from the trend observed from the test data at high velocity regime that the data are questionable at high velocities. The quality of the comparison is limited due to the limited number of actual data points, however, numerical simulations appear to predict fairly accurately the pressure-versus-impact velocity relationship, particularly at low impact-velocity regime.

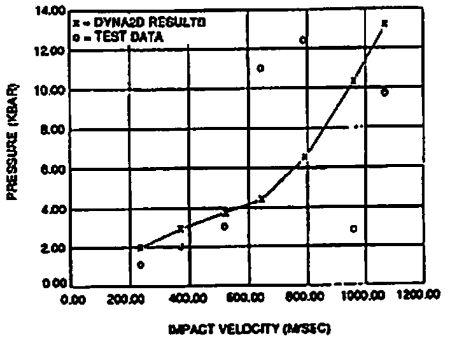

Fig. 7 Impact pressure versus impact velocity

8. Modeling of detonation due to fragment impact

In the study of sympathetic detonation, fragment impact is one of the primary mechanisms that can cause initiation and propagation of detonation. Due to the expense and difficulties in actual large-scale testing of hazardous materials, analytical and numerical techniques have been used to provide insight and guidelines to the design of munitions systems. Starkenberg, et al. 1984 [5], conducted an extensive numerical study of projectile impact shock initiation of bare and covered Composition-B explosive. Bahl, et al. in 1981 [6] correlated numerical modeling results with experiments. Both studies show good correlation between their 2-dimensional computer and physical experiments.

The findings from the numerical simulation effort on an 80-gram FSP impacting a steel plate, which is backed by unconfined cast H6 explosive, are described in this paper. The objective was to develop a better understanding of the detonation phenomenon due to fragment impact and to determine an impact velocity range within which detonation of the H6 explosive will not occur for the defined configuration. A reactive flow model, which characterizes the ignition and growth of detonation for the H6 explosive (Cheng et. al., 1988 [7]), was used to predict detonation of the explosive. This reactive model, built on experimental data and developed by fitting the data to the results obtained from numerical simulations, can provide a reliable prediction of shock initiation of explosives subjected to a wide variety of shock stimuli in various hazard calculations (Bahl, et. al., 1981 [6], Lee, et. al, 1980 [8]).

Simulations were performed for fragment impacts at eight various velocities ranging from 235 to 2,225 m/sec. The flow field and detonation resulting from each impact velocity were evaluated. At low-impact velocities, the impact does not provide enough strong shocks or sustained compression to initiate or propagate the detonation on the H6 explosive. At intermediate-impact velocities (below 1,067 m/sec), initiation occurs at localized region and is due mainly to shocks. At impact velocities at or above 2,225 m/sec, detonation breaks out immediately upon impact as a result of very strong shocks that provide enough strength to initiate the propagation of detonation.

9. Numerical model

On this part of the study, Plexiglas was replaced by cast H6 explosive with everything else remained the same. Both the projectile and the plate which represents the warhead casing are made of 4340 steel with a hardness of Rc=30. They are modeled as isotropic elastic-plastic hydrodynamic material, and the hydrodynamic behavior was governed by a Gruneisen-type equation of state.

10. H6 explosive detonation analysis

Detonation behavior of the bare cast H6 explosive is predicted using the reactive flow model (Cheng, et. al., 1988 [9]) previously developed for the explosive. The development of the ignition and growth reaction model for the cast H6 explosive is detailed in Cheng, et. al, 1988 [7], in which the mathematical form of the ignition and growth reaction rate law was formulated.

The mechanical behavior of the H6 explosive was modeled by an isotropic elastic-plastic hydrodynamic material model (Material Type No. 10 in DYNA2D), and the ignition and growth behavior by the equation of state for the Ignition and Growth of Reaction for High Explosives (EOS-type No. 7 in DYNA2D developed by Tarver and Hallquist, 1981[10], 1985 [11]).

At low- to intermediate-impact velocities, deformation in the fragment and the plate was not severe, therefore, no rezoning was required. Rezoning was required several times for impact velocities of 1,067 and 2,225 m/sec in which cases, deformation was severe.

At low-impact velocities (between 235 and 642 m/sec), the execution time of each analysis was set up to approximately 10 micro-seconds. One can determine if this is adequate by examining plots of fraction of reaction at numerous cells along the centerline of the explosive. If at the end of the solution, the fraction of reaction at the far end begins to flatten out, this means the detonation will stop. Longer execution time is required to observe the propagation of the explosive once it initiates. The time must be adequate to predict stop and propagation of the detonation. In this study, rarefaction phenomenon is not considered, so the solution only goes as far as where the shock wave hits the free boundary, for bare explosives.

The flow field of the explosive due to each fragment impact velocity was examined in order to identify the major factors that contribute to initiation and propagation of detonation or failure of detonation. Pressure contours were plotted at various times to trace the flow fields of the projectile, plate, and explosive. Similarly, the fraction of reaction contours was obtained to determine the amount of reaction for the affection region. To examine the initiation and growth of detonation in the explosive, the pressure time and the fraction of reaction time history plots were obtained.

Table 3 Detonation results obtained from numerical simulation for various impact velocities

Impact Velocity (m/sec)	Detonation
235	No
371	No
520	No
642	No
794	No
961	Some
1,067	Some
2,225	Severe

Using the reactive model in the numerical simulation, detonation (Go) or no detonation (No Go) can be predicted. Table 3 lists the results of the numerical simulations for the various fragment impact velocities considered in this study and detonation is predicted at impact velocity exceeding 2,225 m/sec. Detonation will initiate and grow by a small amount in a small region, but will fail to complete for impact velocities between 642 and 1,067 m/sec. At impact velocities below 642 m/sec, little or no initiation of detonation will occur. The above result was deduced by examining the pressure time and fraction of reaction time history plots at several selected cells along the centerline of the explosive. Figure 8 shows location of the selected cells in the explosive. The pressure and fraction of reaction time history plots for the impact velocity of 2,225 m/sec are shown in Fig. 9 and 10

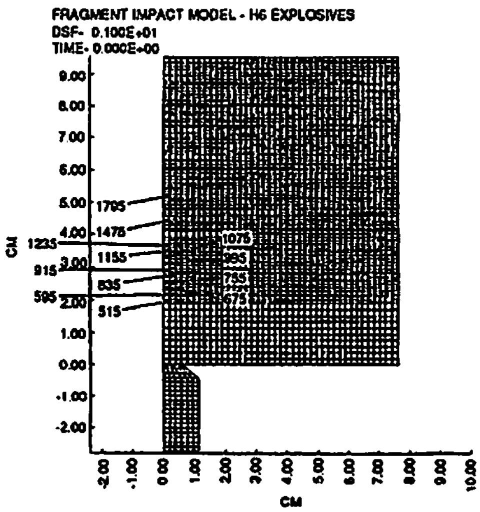

Fig. 8 Locations of selective cells in the explosives for investigating the fractions of reaction and shocks

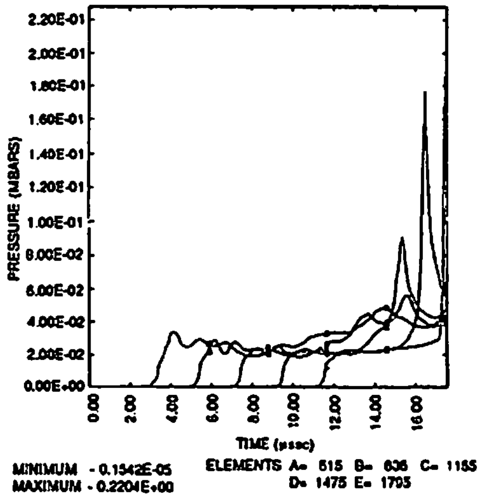

Fig. 9 Pressure history at various elements at impact velocity = 2,225 m/sec

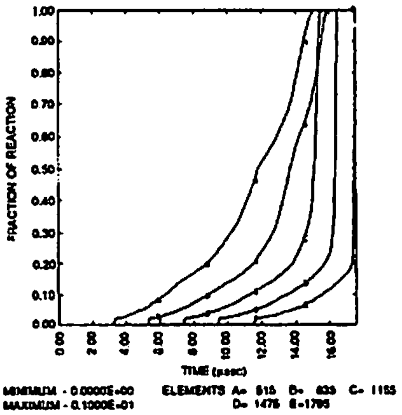

Fig. 10 Fraction of reaction history at various elements at impact velocity = 2,225 m/sec

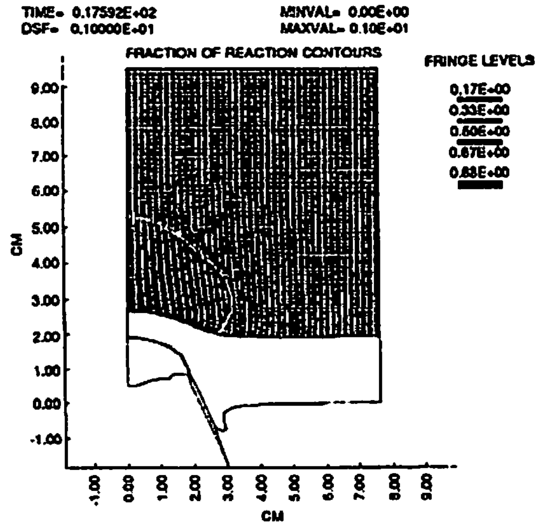

Fig. 11 Fraction of reaction contours in H6 explosives at time = 17.592 μsec for impact velocity = 2,225 m/sec

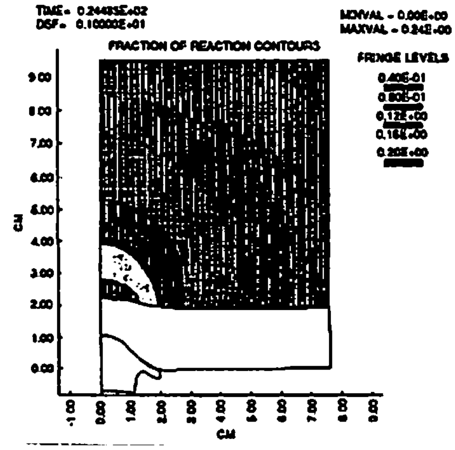

Fig. 12 Fraction of reaction contours in H6 explosives at time = 24.485 μsec for impact velocity = 2,225 m/sec

for impact velocity of 2,225 m/sec, respectively.

As an example to interpret these figures, examine the impact velocity of 2,225 m/sec. The fraction of reaction at all these cells had built up to 100% indicating the continuous propagation of detonation (as shown in Fig. 10). Unless an on-coming neutralizer has resulted from ensuring rarefactions, which may quench the detonation, complete detonation will occur. The results are reinforced by examining the fraction of reaction contours plot at 17.59 micro-seconds (Fig. 11) in the explosive. A large zone in the explosive has developed into 100% of fraction of reaction at 17.59 micro-seconds.

This result is in contrast of that obtained for impact velocity of 961 m/sec in which case detonation has initiated but failed to propagate to a completion. Figure 12 shows a fraction of reaction contour at 24.485 micro-seconds, and detonation has initiated at a small region in the explosive and built up to only about 20%, even when the shock front has reached the boundary of the explosive. Behind the shock front there was not enough reinforcement to develop further propagation of the detonation.

With the aid of time history plots, the following deduction can be formulated:

1. At high-impact velocities, strong shocks developed. The shock pressures are greater than the detonation pressure and therefore, a detonation started immediately. These shocks exhibit enough strength to accelerate the reaction behind the shock-front that move towards the boundary (Johansson, et. al. 1970 [12]). The diameter and the length of the current configuration were both adequate to allow the detonation to become steady. Complete detonation would result.
2. At intermediate-impact velocities, shock pressure exceeded the initiation threshold and detonation ignited. However, the shocks were not strong enough to sustain the propagation and initiation over distance in the explosive. Reaction extended only a very localized region and could build nearly to completion, but the current configuration did not allow the growth of reaction in other areas, so detonation failed to propagate.
3. At low-impact velocities, the energy did not produce high enough shock pressures to initiate or propagate the reaction.

11. H6 Explosive numerical modeling conclusions

Simulations were performed successfully for impacting FSP's on a steel plate that was backed by unconfined cast H6 explosive. Using a previously developed reactive flow model, detonation was predicted to occur at an impact velocity of 2,225 m/sec for the current configuration. Detonation would not initiate for low-impact velocities (below 642 m/sec). At intermediate velocities (between 642 and 1,067 m/sec), detonation would initiate at a very localized region, but would not propagate to severe detonation. Due to the resolution of the specified impact velocities, the critical velocity at which detonation would occur could not be exactly determined, however, it would lie between 1,067 and 2,225 m/sec.

Results obtained from this study provided some insight as to the major factors that could contribute to the detonation (or lack of detonation), and the conclusion drawn from the numerical simulations was valid for the current configuration. Generalization of the result could be allowed to a small degree if the problem of concern do not vary significantly from the current one. However, the results setup as the effects due to boundary and the confinement of the explosive are not accounted for in this study.

Acknowledgements

The authors would like to thank N.S. Brar and Mark Laber in performing the Manganin stress gauge experiments for performing the Manganin stress gauge experiments. We are also grateful to Dr. J.O. Hallquist for his advices in modeling, and to Dr. C.M. Tarver for his advice on the detonation physics and reactive flow model. Appreciation is also going to the FMC Advanced System Center's and Central Engineering Lab's Management for their support of this project back in 1988.

References

1) Brar, N.S., 1988, "Manganin Gauge Ballistic Testing," Final Report to FMC and Martin Marietta Corporation.
2) Rosenberg, Z. and Strader, E., 1985, "Pulsed Constant-Current Power Supply for Dynamic Stress Measurements with In-Material Piezoresistance Gauges," Dayton Impact Physics Research Institute, University of Dayton, Research Report, UDR-TR-85-18.
3) Rosenberg, Z. and Partom, Y., Mayseless, M., and Falcovitz, J., 1984, "Determination of Stress-Time Histories in Axially Symmetric Impacts with the Two Gauge Technique," J. Appl. Phys., Vol. 56, pp. 1434-1439.
4) Hallquist, J.O., 1988, DYNA2D User's Manual, UCID-18756, Rev. 3 (Draft), March 1988.
5) Starkenberg, J., Huang, Y., and Arbuckle, A., 1984, "Numerical Modeling of Projectile Impact Shock Initiation of Bare and Covered Composition-B," Technical Report ARBRL-TR-02576.
6) Bahl, K.L., Vantine, H.C. and Weingarts, R.L., "The Shock Initiation of Bare and Covered Explosives by Projectile Impact," Seventh International Symposium on Detonation, pp. 325-335.

7) Cheng, W.L., 1988, "Development of a Shock Initiation and Propagation of Detonation Model for Cast H6 Explosive for Numerical Modeling of Sympathetic Detonation," FMC Central Engineering Lab. Internal Report MTM# 252-88.
8) Lee, E.L. and Tarver, C.M., 1980, Physical Fluids, 23, 2362.
9) Langlie, S.L. and Cheng, W.L., 1988, "Numerical Modeling of Sympathetic Detonation," PVP-Vol. 134, Shock and Wave Propagation, edited by Shin, Y.S., and Kim, K.S., pp. 59-67.
10) Tarver, C.M. and Hallquist, J.O., 1981, Seventh International Symposium on Detonation, Naval Surface Warfare Center, NSWC MP 82-334, Annapolis, MD, pp. 1029.
11) Tarver, C.M. and Hallquist, J.O., 1985, Eighth International Symposium on Detonation, Naval Surface Warfare Center, NSWC MP 86-294, Annapolis, MD, pp. 951.
12) Johansson, C.H. and Persson, P.A., 1970, Detonics of High Explosives, Academic Press, London and New York, pp. 81.